

RSC Advances



This is an *Accepted Manuscript*, which has been through the Royal Society of Chemistry peer review process and has been accepted for publication.

Accepted Manuscripts are published online shortly after acceptance, before technical editing, formatting and proof reading. Using this free service, authors can make their results available to the community, in citable form, before we publish the edited article. This *Accepted Manuscript* will be replaced by the edited, formatted and paginated article as soon as this is available.

You can find more information about *Accepted Manuscripts* in the [Information for Authors](#).

Please note that technical editing may introduce minor changes to the text and/or graphics, which may alter content. The journal's standard [Terms & Conditions](#) and the [Ethical guidelines](#) still apply. In no event shall the Royal Society of Chemistry be held responsible for any errors or omissions in this *Accepted Manuscript* or any consequences arising from the use of any information it contains.



Journal Name

ARTICLE

Structural and electronic properties of alkali metal peroxides at high pressures

Naihang Deng^a, Wenyong Wang^a, Guochun Yang^{a,b,*}, and Yongqing Qiu^{a*}

keyReceived 00th January 20xx,
Accepted 00th January 20xx

DOI: 10.1039/x0xx00000x

www.rsc.org/

Alkali metal peroxides have a wide range of industrial applications (e.g., energy storage and oxygen source). It is well known that pressure can cause profound structural and electronic changes, leading to the fundamental modification of the physical properties. Here, we reported the structural phase transition, lattice dynamics, and electronic property of alkali metal (Li, Na, K, and Rb) peroxides by using the unbiased structure searching techniques and first-principles density functional calculations in the pressure range of 0-100 GPa. The predicted first-order phase transition pressures in Li₂O₂, Na₂O₂, K₂O₂ and Rb₂O₂ occur at ~84, 28, 7 and 6 GPa, respectively, which closely correlates with the electronegativity of alkali metals. Different phase transition mechanisms and complex phase transition structures have been observed for these alkali metal peroxide compounds. These predicted high-pressure phases are thermodynamically stable against decomposition into alkali metal oxides plus O₂ or alkali metals plus O₂. Interesting, the character of the peroxide group (O₂²⁻) is maintained under the considered pressure range. Phonon calculations using the quasiharmonic approximation confirm that these structures are dynamically stable. The band gaps for the studied alkali metal peroxides increase with increasing pressure. This work provides an opportunity for understanding the structures and electron properties of alkali metal peroxides at high pressures.

1 Introduction

Peroxide is a compound containing an oxygen-oxygen (O-O) single bond,¹ which is named as the peroxide group (O₂²⁻) or peroxy group. The oxygen atoms in the peroxide ion have an oxidation state of -1. In general, peroxide compounds can be divided into organic and inorganic ones. Most of the inorganic peroxides have an ionic, salt-like character, while the organic peroxides are dominated by the covalent bonds. Peroxide compounds are of great significance in diverse fields such as chemistry, medicine, material science, and energy storage. For example, hydrogen peroxide is broadly used as a strong oxidizer, bleaching agent, and disinfectant.^{2, 3} Calcium peroxide (CaO₂) can be used as a source of chemically bound but easily evolved oxygen in fertilisers, in soil remediation, and for oxygenation and disinfection of water.^{4, 5} Lithium peroxide (Li₂O₂) acts as the main discharge product in the Li-air battery with greatly high energy density.⁶⁻⁸ Li₂O₂ is also used as the oxygen source by reacting them with carbon dioxide to produce oxygen and lithium carbonate.⁹ Sodium peroxide (Na₂O₂) also functions as a discharge

product in the Na-air battery or the oxygen source. Very recently, peroxide ion observed in ionic crystals might have a large impact on a range of industrial applications including solid oxide fuel cells.^{10, 11}

It is well known that pressure can cause profound structural change, tune the band gap or induce insulator or semiconductor to metal phase transition.¹²⁻¹⁴ As far as we known, the electronic structure and phase transition of alkali metal peroxides under high pressure have not been investigated. Moreover, specific energy density of the Li-air or Na-air battery greatly exceeds that of a Li ion battery and is aimed as the next-generation battery.¹⁵⁻¹⁸ However the high resistance of Li₂O₂ greatly limits the rate capacity, leads to high charge overpotential, and obstructs the rechargeability of the Li-air battery.¹⁹⁻²² Up to now, only two examples of peroxide compounds were used to investigate the high pressure behavior of peroxide group (e.g. hydrogen peroxide (H₂O₂)²³ and calcium peroxide (CaO₂)^{24, 25}). It is found that the behaviour of peroxide group under pressure strongly correlates with the component element. Specifically, H₂O₂ gradually decomposes into a mixture of H₂O and O₂ above 18 GPa, while peroxide (O₂²⁻) and electronic insulating nature in CaO₂ can be kept in the pressure range of 0-200 GPa. Thus, the investigation of alkali metal peroxides under high pressure also represents a step forward toward the understanding of structure and property of peroxide group.

In this work, we investigated the high-pressure phases of alkali metal peroxides by using unbiased structure searching techniques and first-principles density functional calculations. It is found that the phase transition pressures and structures of alkali metal peroxides strongly depend on electronegativity of alkali metals. The peroxide groups for the studied compounds are maintained under

^aFaculty of Chemistry, Northeast Normal University, Changchun 130024, China.

E-mail: yanggc468@nenu.edu.cn; qiyuq466@nenu.edu.cn

^bState Key Laboratory of Superhard Materials, Jilin University, Changchun 130012, China.

[†]Footnotes relating to the title and/or authors should appear here.

Electronic Supplementary Information (ESI) available: [The dependence of phase pressures and electronegativity for the considered alkali metal peroxides compounds; Variation of the unit cell volume as a function of pressure; Pressure dependence of band gaps for the P6₃mmc and P2₁/c structures in Li₂O₂, and detail structural parameters of the first-order phase transitions]. See DOI: 10.1039/x0xx00000x

the considered pressure range. Increasing the pressure enlarges the band gaps of the considered compounds.

2 Computational details

The structural optimization and electron property calculations were performed in the framework of density functional theory within the Perdew–Burke–Ernzerhof parameterization²⁶ as implemented in the VASP (Vienna ab initio simulation package) code.²⁷ The electron-ion interaction was described by projected-augmented-wave potentials with $2s^1p^0$, $3s^1p^0$, $4s^1p^0$, $5s^1p^0$ and $2s^22p^4$ and as valence electrons for Li, Na, K, Rb and O, respectively. The use of the plane-wave kinetic energy cutoff of 600 eV and Monkhorst–Pack k-meshes with grid spacing of $2\pi \times 0.015 \text{ \AA}^{-1}$ were chosen to ensure that all the enthalpy calculations are well converged to better than 1 meV/atom. The phonon calculations were performed to determine the dynamical stability through supercell method as implemented in the PHONOPY code.²⁸

To search for the possible structures under high pressure, we used the unbiased structure prediction method based on a particles warm optimization algorithm as implemented in the CALYPSO code.^{29,30} The most significant feature of this methodology is the capability of predicting the stable structure with only the

knowledge of the chemical composition. This method has been bench marked on various known systems, ranging from elements to binary and ternary compounds.^{31–35} We perform structure searching with simulation cell sizes of 1 - 4 formula units at pressure of 0, 25, 50, and 100 GPa, respectively. The structure search for the considered compounds converged (evidenced by no structure with the lower enthalpy emerging) after 1000 ~ 1200 structures investigated (i.e. in about 20 ~ 30 generations). Detailed description of the structural predictions can be found in the Supporting Information. We used the VESTA program to illustrate the crystal structures.³⁶

3 Results and discussion

Structure predictions with 1 - 4 formula units (f.u.) per simulation cell were carried out at pressure range of 0 ~ 100 GPa as implemented in the CALYPSO code. The experimental structures at ambient pressure were all successfully reproduced, validating our methodology in application to alkali metal peroxides. For example, the experimental hexagonal structure of Li_2O_2 (space group $P6_3/mmc$, 2 f.u. per cell) was successfully reproduced. Moreover, the optimized lattice parameters are $a = 3.16 \text{ \AA}$ and $c = 7.68 \text{ \AA}$, respectively,

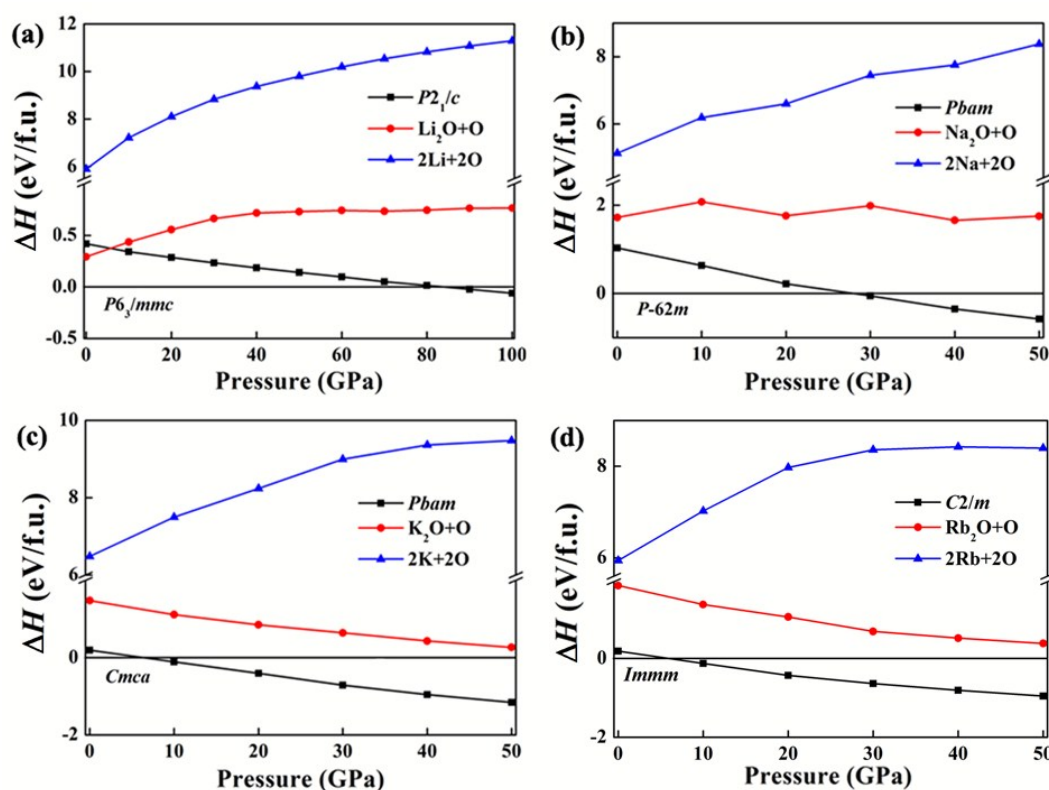


Fig. 1 The relative enthalpy per formula unit as a function of pressure within PBE calculations at $T = 0 \text{ K}$ for the studied alkali metal peroxides. (a) Li_2O_2 with respect to $P6_3/mmc$ structure in the pressure range of 0-100 GPa. (b) Na_2O_2 is relative to $P-62m$ structure for the pressure regime between 0 and 50 GPa. (c) and (d). K_2O_2 and Rb_2O_2 with respect to $Cmca$ and $Immm$ structures, respectively. Other structures with relative lower enthalpies can be found in the supporting information (Fig. S2-S5).

which are in excellent agreement with the experimental values of 3.14 and 7.65 Å,³⁷ and 3.16 and 7.69 Å from other theoretical calculations,²¹ giving a strong support on the validity of our adopted pseudopotential and functional. The calculated enthalpies per formula unit as a function of pressure were shown in Fig. 1. The specific phase transition structures and properties will be discussed individually, but it is first desirable to make general description for all the considered compounds. It is found that the first-order phase transition pressures have been found for Li₂O₂ (84 GPa), Na₂O₂ (28 GPa), K₂O₂ (7 GPa) and Rb₂O₂ (6 GPa), respectively, which decreases with decreasing the electronegativity of alkali metals. That is, the smaller electronegativity, the lower phase transition pressure (Fig. S1). With decreasing the electronegativity, atomic nucleus gradually weakens the attractive of the outer electrons. Thus, the elements with smaller electronegativity are easier compressed and have higher compressibility. Similar trends have been observed in the

IIIA–VA compounds³⁸ and alkali metal hydrides.^{39,40} The peroxide groups for all considered compounds are maintained in the pressure range of 0–100 GPa. In addition, the studied compounds upon phase transition exhibit complex structural characters as will be discussed later. It should be noted that these structures are thermodynamically stable with respect to the decomposition into alkali metal oxides + O₂ or alkali metals + O₂ (Fig. 1).

Li₂O₂ has the hexagonal structure (space group *P6₃/mmc*) at ambient pressure. This hexagonal phase transforms to a monoclinic (space group *P2₁/c*) form at 84 GPa. The O–O bond length in the peroxide group is 1.45 Å at the phase transition pressure, which is slightly shorter the distance (1.55 Å) at ambient pressure, while is greatly longer than that of superoxide (1.33 Å).⁴¹ This indicates that the peroxide group is maintained upon the pressure-induced phase transition. Although the two phases have the same Li–O

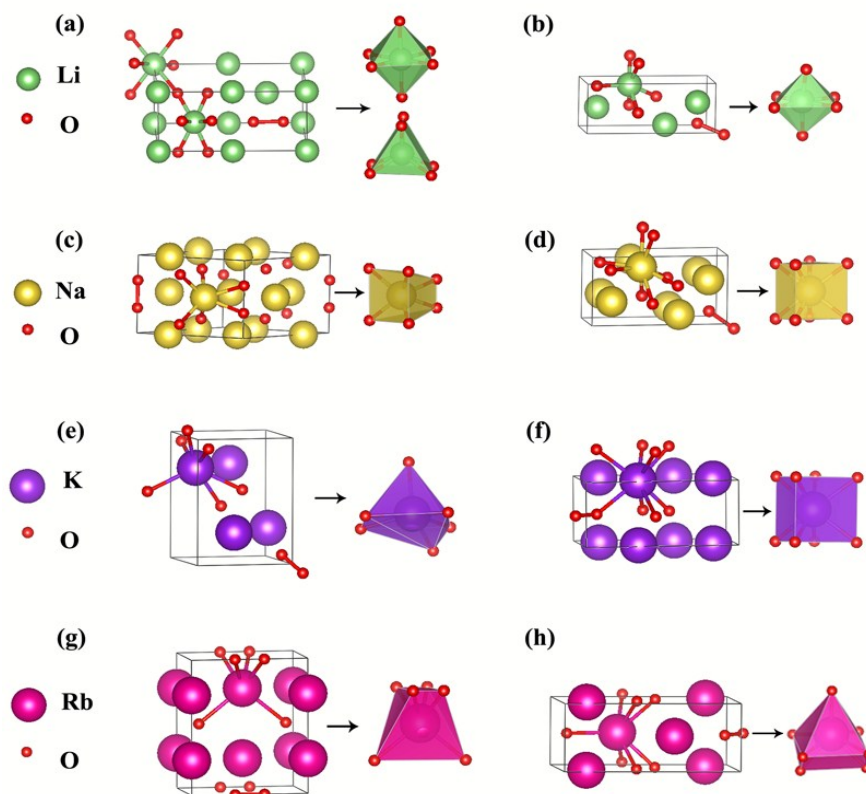


Fig. 2 Crystal structures at ambient pressure (left) and first-order phase transition pressure (right). (a) Li₂O₂ in *P6₃/mmc* structure at 0 GPa. (b) Li₂O₂ in *P2₁/c* structure at 84 GPa. (c) Na₂O₂ in *P-62m* structure at 0 GPa. (d) Na₂O₂ in *Pbam* structure at 28 GPa. (e) K₂O₂ in *Cmca* structure at 0 GPa. (f) K₂O₂ in *Pbam* structure at 7 GPa. (g) Rb₂O₂ in *Immm* structure at 0 GPa. (h) Rb₂O₂ in *C2/m* structure at 6 GPa.

coordination number of six, the average Li-O distance 1.809 Å in $P2_1/c$ structure is greatly shortened compared with 2.081 Å in $P6_3/mmc$ structure. Atomic charges obtained from the Bader or Mulliken charge analysis are nearly same between the two phases (Table S1.). In other words, there is little effect on the charge distribution upon this phase transition. As a consequence, coulomb interactions are strengthened in the high pressure phase. In addition, this phase transition reduces the volume by $\sim 2.9\%$ relative to the $P6_3/mmc$ structure (Fig. S6), which also lowers the enthalpy. Based above analysis, this phase transition mechanism can attribute to the increase of coulomb interaction between Li and O atoms and the decrease of the volume.

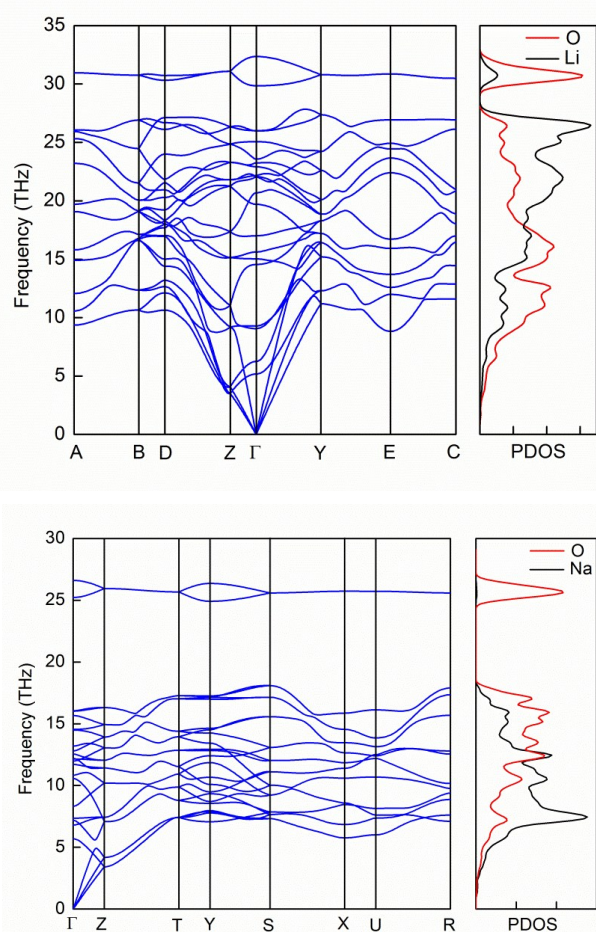


Fig. 3 Phonon dispersion curve (blue) and partial phonon density of states (PDOS) for Li_2O_2 (top) in the $P2_1/c$ structure and Na_2O_2 (bottom) in the $Pbam$ structure, respectively.

Although Na_2O_2 and K_2O_2 have different structures (hexagonal and tetragonal) at ambient pressure, they are transformed to

orthogonal structures (space group $Pbam$) under pressures. The distances between the two nearest oxygen atoms for Na_2O_2 and K_2O_2 are 1.510 and 1.531 Å at phase transition pressure, which are comparable to 1.515 and 1.525 Å at ambient pressure, respectively. It is mentioned that the peroxide groups are also maintained in the two compounds. It is found that the average Na-O distance 2.215 Å in orthogonal structure is only slightly shorter than 2.226 Å of the hexagonal structure, which is obviously different from the observation in Li_2O_2 . The Na-O coordination number is changed from 6 to 8 and volume is greatly reduced by $\sim 12.47\%$ upon the phase transition (Fig. S6). The similar results can be found in K_2O_2 . Therefore, this phase transition mechanism is attributed to the higher coordination and denser polyhedra packing.

For the Rb_2O_2 , tetragonal structure ($Immm$) is transformed to monoclinic one (space group $C2/m$) at 6 GPa. Upon these transitions, the O-O distance in the peroxide group becomes slightly shorter than that of ambient pressure structure, but is still longer than that of superoxide group. The Rb-O coordination number is changed from 6 to 7 and volume is reduced by $\sim 7.85\%$ upon this phase transition (Fig. S6). Moreover, the average Rb-O distance is comparable to that of ambient pressure structure. Thus, this phase transition mechanism is similar to that of Na_2O_2 or K_2O_2 .

To assess the dynamic stability of the predicted phases, the quasi-harmonic model was adopted to calculate the phonon spectra using the supercell method. No imaginary phonon frequency confirms the dynamic stability of these predicted phases (Fig. 3 and Fig. S7). For the Li_2O_2 in the $P2_1/c$ structure, the motion of the O ions mainly dominates the vibrational states in the high and low frequency regimes, while the coupling Li-O pairs in the lattices contributes to the middle frequency regimes, which is similar to the vibrational character of Li_2O_2 in the $P6_3/mmc$ structure at ambient pressure.⁴² For the highest vibrational frequency (~ 35 THz), the strong and sharp peak of the O partial phonon density of states appears to be due to the O-O stretching mode, which again indicated its existence the peroxide group. In addition, the phonon bands in the low frequency region substantially broaden as a result of the shorter Li-O distance. The vibrational characters of Na_2O_2 , K_2O_2 , and Rb_2O_2 (Fig. S7) are similar to those of Li_2O_2 in the $P2_1/c$ structure, while the vibrational frequency of Na_2O_2 and K_2O_2 is much lower than that of Li_2O_2 . This might originate from the heavier atomic mass and longer O-O distances in Na_2O_2 , K_2O_2 , and Rb_2O_2 .

To understand the electronic structure and nature upon the phase transition, we calculated the electronic band structure and the projected density of states (PDOS). The ambient pressure phases are also calculated for comparison (Fig. 4). Firstly, Li_2O_2 was taken as an example to investigate the effect of pressure on

the band gaps for $P6_3/mmc$ and $P2_1/c$ structures, respectively (Fig. S8). It is noted that DFT calculation usually underestimates the band gaps. The band gaps of both structures gradually increase with increasing pressure. Thus, Li_2O_2 remains the insulating characters under the considered pressures range as observed in CaO_2 .²⁵ This character is not favorable to enhance the electrical conductivity of Li_2O_2 . The other studied compounds also exhibit similar band gaps variable trend. In other words, the band gaps of the studied compounds increases with increasing the pressure. It is noted that the band gaps decrease with decreasing the electronegativity of alkali metal ($\text{Li}_2\text{O}_2 < \text{Na}_2\text{O}_2 < \text{K}_2\text{O}_2 < \text{Rb}_2\text{O}_2$). There is a common character for the considered compounds: both valence band and conduction band are predominantly O 2p in character, with a small contribution from the Li 2p components.

Structural changes and electronic properties for alkali metal peroxides (Li_2O_2 , Na_2O_2 , K_2O_2 and Rb_2O_2) under pressure have been explored over the pressure range 0-100 GPa. Their phase transition pressures decrease with decreasing the electronegativity of the alkali metals. It is interesting to find that the peroxide group is maintained under the considered pressure range, which is firstly reported in this study. These predicated high-pressure phases are thermodynamically stable against decomposition into alkali metal oxides plus O_2 or alkali metals plus O_2 . Calculation of phonon frequencies on these predicted phases confirm their dynamical stability. Their band gaps become larger with the pressure. This work might provide useful route for experimental investigation on the structure and electron property of alkali metal peroxides under high pressure.

4 Conclusions

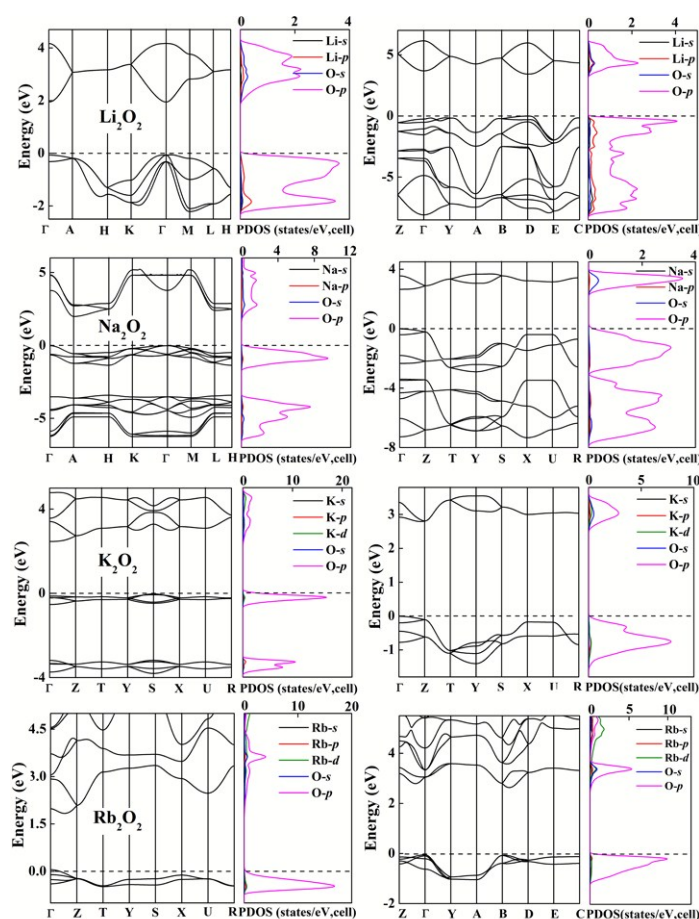


Fig. 4 Electronic band structure and projected density of states (DOS) at ambient pressure (left) and first-order phase transition pressure (right). The dashed line indicates the calculated fermi energy.

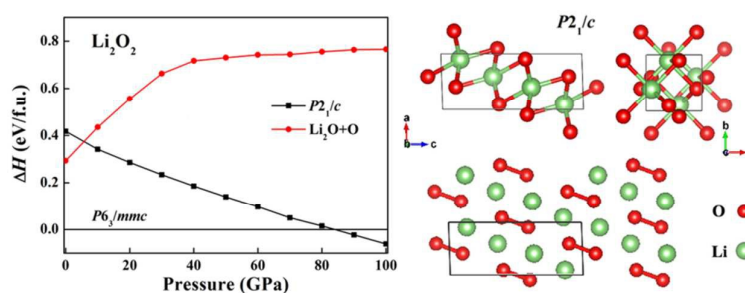
Acknowledgements

The authors gratefully acknowledge financial support from the National Natural Science Foundation of China (21573037 and 21173035) and the Natural Science Foundation of Jilin Province (20150101042JC) and the Postdoctoral Science Foundation of China under grant 2013M541283.

Notes and references

1. A. D. McNaught and A. Wilkinson, *Compendium of Chemical Terminology*, 2nd ed. (the "Gold Book") (1997). ISBN 0865426848.
2. O. Y. Ozyilmaz, T. Yavuz, T. Sari, F. Aykent and A. N. Ozturk, *J. Adhes. Sci. Technol.*, 2015, **29**, 1572-1580.
3. A. M. D. P. Deshpande, T. S. C. M. B. A. Mana, J. L. B. S. Cadnum, A. C. B. S. Jencson, B. M. S. Sitzlar, D. Fertelli, K. B. S. Hurless, S. M. D. M. S. Kundrapu, V. C. K. M. D. M. S. Sunkesula and C. J. M. D. Donskey, *Infection Control and Hospital Epidemiology*, 2014, **35**, 1414-1416.
4. Y. Qian, X. Zhou, Y. Zhang, W. Zhang and J. Chen, *Chemosphere*, 2013, **91**, 717-723.
5. I. A. Massalimov, A. U. Shayakhmetov and A. G. Mustafin, *Russ J Appl Chem*, 2010, **83**, 1794-1798.
6. K. M. Abraham and Z. Jiang, *J. Electrochem. Soc.*, 1996, **143**, 1-5.
7. T. Ogasawara, A. Débart, M. Holzapfel, P. Novák and P. G. Bruce, *J. Am. Chem. Soc.*, 2006, **128**, 1390-1393.
8. B. D. McCloskey, D. S. Bethune, R. M. Shelby, G. Girishkumar and A. C. Luntz, *J. Phys. Chem. Lett.*, 2011, **2**, 1161-1166.
9. Greenwood, Norman N.; Earnshaw, Alan (1984). *Chemistry of the Elements*. Oxford: Pergamon Press. p. 98. ISBN 0-08-022057-6.
10. S. C. Middleburgh, I. Karatchevtseva, B. J. Kennedy, P. A. Burr, Z. Zhang, E. Reynolds, R. W. Grimes and G. R. Lumpkin, *J. Mater. Chem. A*, 2014, **2**, 15883-15888.
11. S. C. Middleburgh, K. P. D. Lagerlof and R. W. Grimes, *J. Am. Ceram. Soc.*, 2013, **96**, 308-311.
12. H. Dekura, T. Tsuchiya, Y. Kuwayama and J. Tsuchiya, *Phys. Rev. Lett.*, 2011, **107**, 045701.
13. L. Hromadová, R. Martoňák and E. Tosatti, *Phys. Rev. B*, 2013, **87**, 144105.
14. Z. Zhao, S. Wang, H. Zhang and W. L. Mao, *Phys. Rev. B*, 2013, **88**, 024120.
15. Y. Chen, S. A. Freunberger, Z. Peng, O. Fontaine and P. G. Bruce, *Nat Chem*, 2013, **5**, 489-494.
16. M. S. Dresselhaus and I. L. Thomas, *Nature*, 2001, **414**, 332-337.
17. Y.-X. Yin, S. Xin, Y.-G. Guo and L.-J. Wan, *Angew. Chem. Int. Ed.*, 2013, **52**, 13186-13200.
18. K. A. See, M. Leskes, J. M. Griffin, S. Britto, P. D. Matthews, A. Emly, A. Van der Ven, D. S. Wright, A. J. Morris, C. P. Grey and R. Seshadri, *J. Am. Chem. Soc.*, 2014, **136**, 16368-16377.
19. C. Laoire, S. Mukerjee, E. J. Plichta, M. A. Hendrickson and K. M. Abraham, *J. Electrochem. Soc.*, 2011, **158**, A302-A308.
20. P. Albertus, G. Girishkumar, B. McCloskey, R. S. Sánchez-Carrera, B. Kozinsky, J. Christensen and A. C. Luntz, *J. Electrochem. Soc.*, 2011, **158**, A343-A351.
21. M. D. Radin, J. F. Rodriguez, F. Tian and D. J. Siegel, *J. Am. Chem. Soc.*, 2012, **134**, 1093-1103.
22. V. Viswanathan, K. S. Thygesen, J. S. Hummelshøj, J. K. Nørskov, G. Girishkumar, B. D. McCloskey and A. C. Luntz, *J. Chem. Phys.*, 2011, **135**, 214704.
23. J.-Y. Chen, M. Kim, C.-S. Yoo, D. M. Dattelbaum and S. Sheffield, *J. Chem. Phys.*, 2010, **132**, 214501.
24. M. Königstein, A. A. Sokol and C. R. A. Catlow, *Phys. Rev. B*, 1999, **60**, 4594-4604.
25. J. R. Nelson, R. J. Needs and C. J. Pickard, *PCCP*, 2015, **17**, 6889-6895.
26. J. P. Perdew, J. A. Chevary, S. H. Vosko, K. A. Jackson, M. R. Pederson, D. J. Singh and C. Fiolhais, *Phys. Rev. B*, 1992, **46**, 6671-6687.
27. G. Kresse and J. Furthmüller, *Phys. Rev. B*, 1996, **54**, 11169-11186.
28. A. Togo, F. Oba and I. Tanaka, *Phys. Rev. B*, 2008, **78**, 134106.
29. Y. Wang, J. Lv, L. Zhu and Y. Ma, *Phys. Rev. B*, 2010, **82**, 094116.
30. Y. Wang, J. Lv, L. Zhu and Y. Ma, *Comput. Phys Commun.*, 2012, **183**, 2063-2070.
31. Y. Wang, H. Liu, J. Lv, L. Zhu, H. Wang and Y. Ma, *Nat Commun*, 2011, **2**, 563.
32. L. Zhu, H. Liu, C. J. Pickard, G. Zou and Y. Ma, *Nat Chem*, 2014, **6**, 644-648.
33. J. Lv, Y. Wang, L. Zhu and Y. Ma, *Phys. Rev. Lett.*, 2011, **106**, 015503.
34. G. Yang, Y. Wang and Y. Ma, *J. Phys. Chem. Lett.*, 2014, **5**, 2516-2521.
35. G. Yang, S. Shi, J. Yang and Y. Ma, *J. Mater. Chem. A*, 2015, **3**, 8865-8869.
36. K. Momma and F. Izumi, *J. Appl. Crystallogr.* 2008, **41**, 653-658.
37. H. Föppl, *Z. Anorg. Allg. Chem.*, 1957, **291**, 12-50.
38. A. Mujica, A. Rubio, A. Muñoz and R. J. Needs, *Rev Mod Phys*, 2003, **75**, 863-912.
39. J. Hooper, P. Baettig and E. Zurek, *J. Appl. Phys.*, 2012, **111**, 112611.
40. A. Shamp, P. Saitta and E. Zurek, *Phys. Chem. Chem. Phys.*, 2015, **17**, 12265-12272.
41. G. F. Carter and D. H. Templeton, *J. Am. Chem. Soc.*, 1953, **75**, 5247-5249.
42. K. C. Lau, L. A. Curtiss and J. Greeley, *J. Phys. Chem. C*, 2011, **115**, 23625-23633.

Table of Contents Graphic



Text for TOC: Different phase transition mechanisms and complex phase transition structures have been observed for the alkali metal peroxide compounds (Li_2O_2 , Na_2O_2 , K_2O_2 , and Rb_2O_2). Moreover, phase transition pressures of the studied metal peroxide compounds closely correlate with the electronegativity of alkali metals. This work provides an opportunity for fully understanding the structures and electron properties of alkali metal peroxides at high pressures.